Remote Sensing of Environment 113 (2009) 2356–2365

Contents lists available at ScienceDirect

Remote Sensing of Environment

journal homepage: www.elsevier.com/locate/rse

Integrated analysis of PALSAR/Radarsat-1 InSAR and ENVISAT altimeter data for mapping of absolute water level changes in Louisiana wetlands

Jin-Woo Kim [a], Zhong Lu [b], Hyongki Lee [a,*], C.K. Shum [a], Christopher M. Swarzenski [c], Thomas W. Doyle [d], Sang-Ho Baek [e]

[a] Division of Geodetic Science, School of Earth Sciences, The Ohio State University, Columbus OH, USA
[b] U.S. Geological Survey, Vancouver WA, USA
[c] U.S. Geological Survey, Louisiana Water Science Center, Baton Rouge LA, USA
[d] U.S. Geological Survey, National Wetlands Research Center, Lafayette LA, USA
[e] Department of Civil Engineering and Environmental Sciences, Korea Military Academy, Seoul, South Korea

ARTICLE INFO

Article history:
Received 4 March 2009
Received in revised form 17 June 2009
Accepted 20 June 2009

Keywords:
InSAR
Satellite radar altimetry
Wetland
Absolute water level change

ABSTRACT

Interferometric Synthetic Aperture Radar (InSAR) has been used to detect relative water level changes in wetlands. We developed an innovative method to integrate InSAR and satellite radar altimetry for measuring absolute or geocentric water level changes and applied the methodology to remote areas of swamp forest in coastal Louisiana. Coherence analysis of InSAR pairs suggested that the HH polarization is preferred for this type of observation, and polarimetric analysis can help to identify double-bounce backscattering areas in the wetland. ENVISAT radar altimeter-measured 18-Hz (along-track sampling of 417 m) water level data processed with regional *stackfile* method have been used to provide vertical references for water bodies separated by levees. The high-resolution (~40 m) relative water changes measured from ALOS PALSAR L-band and Radarsat-1 C-band InSAR are then integrated with ENVISAT radar altimetry to obtain absolute water level. The resulting water level time series were validated with *in situ* gauge observations within the swamp forest. We anticipate that this new technique will allow retrospective reconstruction and concurrent monitoring of water conditions and flow dynamics in wetlands, especially those lacking gauge networks.

1. Introduction

Modern landscapes are highly fragmented based on ownership priorities and land-use preferences. The Lower Mississippi River valley is an important economic corridor of agricultural, fisheries, forestry, and oil and gas enterprises that have contributed to a highly dissected landscape of natural and built levees and dredged canals aiding access, transport, and flood control. Efforts to reconnect dissected parcels into larger conservation planning units for the benefit of wildlife and floodway management require more comprehensive knowledge of how water resources are stored and exchanged between these segregated land units. In most cases, knowledge of water levels and flow patterns is lacking due to insufficient monitoring or gauge equipment on private and public lands within floodplain settings. Existing gauge networks maintained by State and Federal agencies are almost exclusively placed in navigable rivers and rarely in backswamp areas behind flood control levees. Only in recent decades have wetland scientists realized the lack of hydrological coupling in adjoining land units within and between floodways and the need for explicit monitoring of backswamp water levels. Unfortunately, the resources are lacking to deploy and maintain extensive gauge networks that would improve our understanding of the hydrological coupling within highly dissected floodplain settings.

The Lower Atchafalaya River basin is a major distributary diverting nearly 30% of the Mississippi River flow through forested and marsh wetlands at the coastal margin of the Gulf of Mexico. During high floods these wetlands receive nutrient-enriched river water that is believed to be beneficial for plant growth and for reducing the nutrient load that contributes to offshore hypoxia. Because these wetlands are also near sea-level in upper estuary settings, they are also prone to meteorological tides and surge events from landfalling tropical storms. Remote satellite telemetry observations are being used to interpret water level conditions in oceanic and inland settings. Forest cover and habitat type complicate the ability to use any one remotely sensed platform or instrument for accurate water level reconstructions. New methodologies and protocols are needed to use combined remotely sensed observations to improve our ability to monitor continuous water level or distinguish habitat type or other characteristics of wetland environments.

* Corresponding author. Division of Geodetic Science, School of Earth Sciences, The Ohio State University, 275 Mendenhall Laboratory, 125 South Oval Mall, Columbus, OH 43210, USA. Tel.: +1 614 292 2269; fax: +1 614 292 7688.
E-mail address: lee.2444@osu.edu (H. Lee).

0034-4257/$ – see front matter © 2009 Elsevier Inc. All rights reserved.
doi:10.1016/j.rse.2009.06.014

Interferometric Synthetic Aperture Radar (InSAR) has been proven to be useful to measure centimeter-scale water level changes over the floodplain. The L-band SAR satellites such as Shuttle Imaging Radar-C (SIR-C) and Japanese Earth Resources Satellite 1 (JERS-1) were utilized for detecting water changes within the Amazon floodplain (Alsdorf et al., 2000, 2001), and Everglades wetlands in Florida (Wdowinski et al., 2004). Furthermore, the C-band SAR images from European Remote Sensing satellite (ERS-1/2) and Radarsat-1 were used for revealing water changes beneath Louisiana swamp forests, and it has been shown that polarization was an important factor in wetland application as Radarsat-1 images with horizontal-transmit and horizontal-receive (HH) polarization were more coherent than ERS-1/2 images with vertical-transmit and vertical-receive (VV) polarization over the swamp forests (Lu et al., 2005; Lu & Kwoun, 2008). This is based on the fact that the water beneath the swamp forest can provide double-bounce backscattering, which allows InSAR coherence to be maintained. Over the past few years, satellite radar altimetry has also been successfully used for water level monitoring over large inland water bodies such as the Great Lakes (Morris & Gill, 1994; Birkett, 1995) and the Amazon Basin (Birkett, 1998; Birkett et al., 2002), which have higher chances to be processed as ocean-like radar return. However, significant amount of data loss can occur during the periods of stage minima (lowest water level) due to the interruptions to the water surface by the surrounding topography. Furthermore, the radar return from a relatively small water body can be distorted. These limitations can be overcome by retracking individual return waveform (Berry et al., 2005; Frappart et al., 2006). Specifically, wetland water level variation beneath various types of vegetation (e.g., swamp forest, saline marsh, brackish marsh) in coastal Louisiana has been monitored using retracked TOPEX/POSEIDON radar altimetry with an aid of 10-Hz *stackfile* procedure (Lee et al., 2009).

In this study, we utilized Phased Array type L-band Synthetic Aperture Radar (PALSAR) and C-band Radarsat-1 SAR images, and ENVIronmental SATellite (ENVISAT) radar altimetry data together for the water level monitoring beneath the swamp forest in the Atchafalaya Basin (Fig. 1). Differential InSAR (D-InSAR) method can provide relative water level changes with high spatial resolution (~40 m), but a vertical reference is necessary to convert these to absolute water level changes. Most *in situ* water level gauges are located not in the swamp forests, but in the river channel; thus they cannot be used to resolve the absolute water level changes beneath the swamp forest. However, it has been shown that radar altimetry can provide absolute water level changes along its high-rate (10-Hz for TOPEX, 18-Hz for ENVISAT, corresponds to along-track sampling of 750 m and 417 m, respectively) nominal ground track (Lee et al., 2009). Hence, it can be used as the geocentric reference to enable estimation of the absolute water level changes. Finally, we then verified this technique using *in situ* water level gauges located within the swamp forest.

2. Data

For InSAR processing, eight scenes of PALSAR L-band and four scenes of Radarsat-1 C-band are used, as given in Table 1. Six scenes among the PALSAR scenes and all Radarsat-1 scenes are HH polarized, and the other two PALSAR scenes are horizontal-transmit and vertical-receive (HV) polarized. As illustrated in Fig. 1, the SAR images cover southeastern Louisiana, which consists of swamp forests, marsh, upland forests, and agricultural field. The incidence angles of PALSAR and Radarsat-1 scenes are approximately 38.7° from descending track and 27.6° from ascending track, respectively. PALSAR and Radarsat-1 have different wavelengths (PALSAR: 23.62 cm, Radarsat-1: 5.66 cm). As shown in Table 1, we used Radarsat-1 InSAR pair with perpendicular baselines shorter than 400 m because longer perpendicular baseline can result in loss of coherence. However, the coherence was still maintained using PALSAR InSAR pairs with relatively longer baselines. Pairs 3 and 4 in Table 1 were used to compare the coherences obtained from HH and HV polarizations.

The ENVISAT altimeter data used in this study are from the periods of September 2002 to July 2008. The ENVISAT orbits on a 35-day repeat cycle with 98.5° inclination. The ENVISAT Geophysical Data Record (GDR) contains 18-Hz retracked measurements, corresponding to a ground spacing of approximately 417 m. The instrument corrections, media corrections (dry troposphere correction, wet troposphere correction calculated by the French Meteorological Office (FMO) from the European Centre for Medium-Range Weather Forecasts (ECMWF) model, and the ionosphere correction based on Global Ionosphere Maps (GIM)), and geophysical corrections (solid Earth tide and pole tide) have been applied. The ionosphere corrections usually obtained by combining the dual-frequency altimeter measurement over ocean could not be used in this study because of land contaminations. Thus, the GIM ionosphere corrections, based on Total Electron Content (TEC) grids, in the GDR were used for this study. Additionally, the 5.6 m level Ultra Stable Oscillator (USO) anomalies for ENVISAT cycles 44–70 were corrected using the European Space Agency's (ESA) algorithm in the form of a table (Benveniste, 2002).

3. Methodology

Two-pass D-InSAR method utilizes two SAR images acquired at different times over the same area. The interferometric phase difference (ϕ) between two SAR images, called interferogram, includes the signatures by topography (ϕ_{topo}), displacement (ϕ_{disp}), atmosphere effect (ϕ_{atmo}), baseline error (ϕ_{baseline}) and noise (ϕ_{noise}) such as:

$$\phi = \phi_{\text{topo}} + \phi_{\text{disp}} + \phi_{\text{atmo}} + \phi_{\text{baseline}} + \phi_{\text{noise}}. \quad (1)$$

By removing other components, the phase difference by displacement can be acquired. Topographic phase can be simulated from a Digital Elevation Model (DEM). The atmospheric effects can introduce spatially-correlated artifacts of a few centimeters, and the baseline error can be modeled and removed. The noise level of the interferometric phase depends on the coherence of the image pairs. In general, the volume and surface scattering over forested areas yield low coherence or decorrelation (loss of coherence). However, if the emitted radar signal is reflected twice from the water surface and vegetation, and returned back to the antenna, which is called "double-bounce" backscattering, it is possible to obtain a good coherence from inundated vegetation. As a result, the water level change ∂h can be obtained from the displacement phase as follows:

$$\partial h = -\frac{\lambda \phi_{\text{disp}}}{4\pi \cos\theta_{\text{inc}}} + n \quad (2)$$

where λ is the SAR wavelength, θ_{inc} is the SAR incidence angle, and n is the noise caused by the decorrelation effects (Lu & Kwoun, 2008).

It is important to note that the InSAR technique cannot detect spatially homogeneous water level changes (Lu & Kwoun, 2008; Lu et al., 2009). For instance, the water levels at two locations, x_0 and x_1 can increase homogeneously as much as ∂h ($=h_1-h_0$) during a time interval, ∂t (Fig. S1(a), Supplementary material). In this case, the InSAR method cannot measure any water level changes unambiguously because it can only measure the phase difference between a pixel and the neighboring pixels from which only the relative surface displacement (Lu, 2007), which is zero in this case, can be estimated. On the other hand, when the water levels at two locations vary heterogeneously in space during the time interval ∂t (Fig. S1(b), Supplementary material), the relative water level change between two locations, or the gradient of the water level change $\left(\frac{\partial h / \partial t}{\partial x}\right)$ can be measured from the interferogram. However, the absolute water level

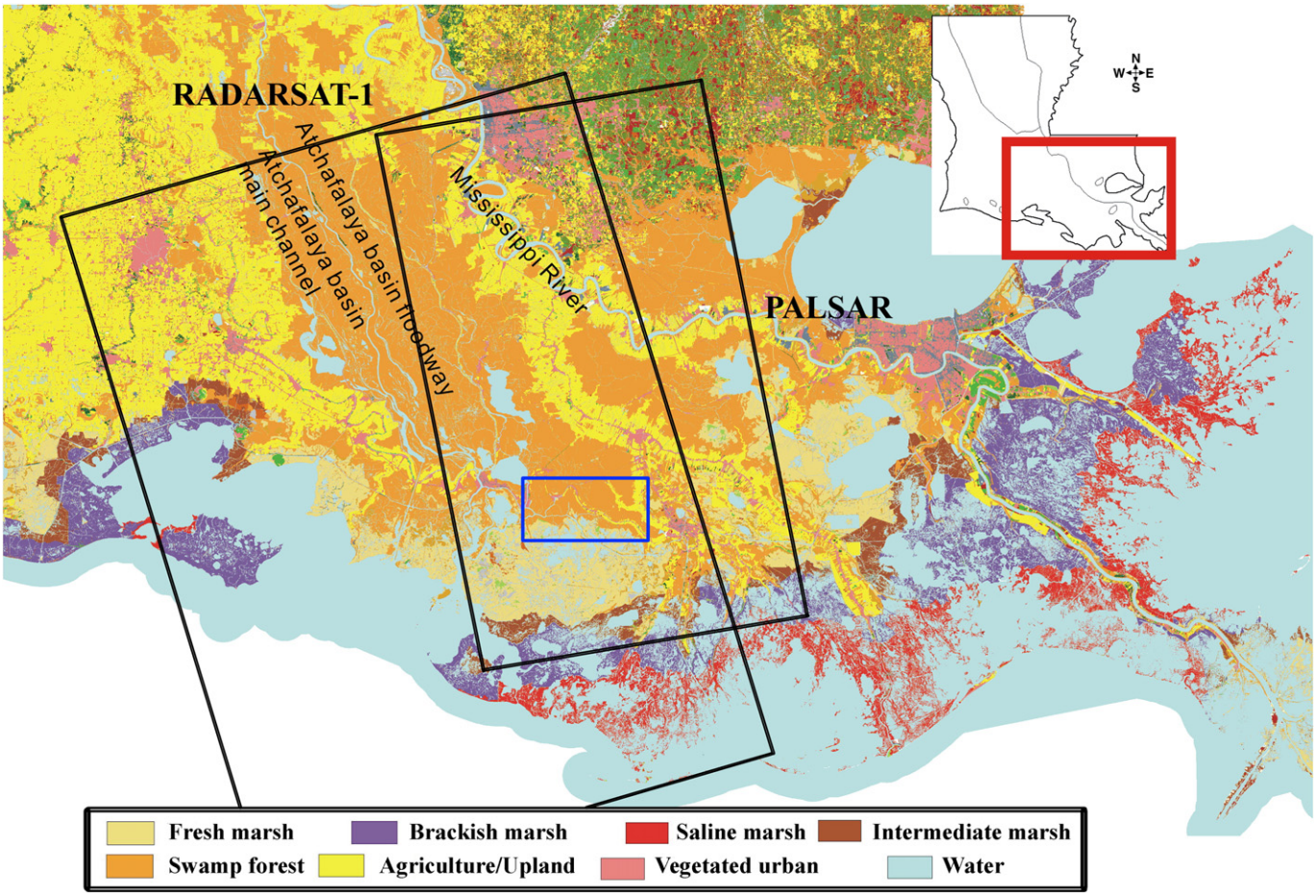

Fig. 1. Thematic map, modified from Gap Analysis Program (GAP) and 1990 U.S. Geological Survey National Wetlands Research Center (USGS-NWRC) classification results, showing major land cover classes of the study area. Polygons represent extents of InSAR images shown in Table 1 for the PALSAR and Radarsat-1 tracks, respectively.

changes, dh_0/dt at x_0 and dh_1/dt at x_1, cannot be derived from the InSAR measurement alone. As a result, the water level measurement at a location within the interferogram is necessary to convert the relative water level change into the absolute water level change. The conversion can be achieved from Eq. (3) such as:

$$\begin{bmatrix} \dfrac{dh_1}{dt} = \dfrac{dh_0}{dt} + \dfrac{\partial h_1/\partial t}{\partial x}\Delta x + \dfrac{\partial h_1/\partial t}{\partial y}\Delta y + \varepsilon \\ \vdots \\ \dfrac{dh_n}{dt} = \dfrac{dh_0}{dt} + \dfrac{\partial h_n/\partial t}{\partial x}\Delta x + \dfrac{\partial h_n/\partial t}{\partial y}\Delta y + \varepsilon \end{bmatrix} \tag{3}$$

where dh_n/dt is the absolute water level change at the nth location, dh_0/dt is the absolute water level change at location x_0 obtained from a gauge station or altimeter measurement to be used as the vertical reference, $\frac{\partial h_n/\partial t}{\partial x}$ and $\frac{\partial h_n/\partial t}{\partial y}$ are the gradients of the water level change (relative water level changes) in x and y directions obtained from the InSAR measurement, and ε is an additional error term due to inappropriate observation of radar altimetry or the gradient error of InSAR. Although the water level gauge can be an ideal source providing the absolute water level change to be used as the vertical reference, most gauges are located in the river channel, not in the swamp forest. Due to the fact that the water level change in the swamp forest can be different from that in the river channel (Lu et al., 2005; Lu & Kwoun, 2008), the water level gauges in the river channel are not appropriate to be used as the vertical reference in this study.

Instead, the geocentric water level change measured from satellite radar altimetry can be used as the vertical reference. Along each 18-Hz ENVISAT nominal ground track (or *bin*), the absolute water level change time series can be generated from the ICE-1 retracked (Bamber, 1994) ENVISAT measurements with the regional *stackfile* method (for details, see Lee et al., 2008, 2009). Hence, the radar altimeter, which passes over the swamp forest, can provide several observations of absolute water level changes denoted as $\left(\frac{dh_0}{dt}\right)_1, \cdots, \left(\frac{dh_0}{dt}\right)_n$ in Fig. S2,

Table 1
Characteristics of PALSAR/Radarsat-1 InSAR pairs.

Pair	Master date	Slave date	Sensor	Polarization	Temporal baseline (days)	Perpendicular baseline (m)
1	2007.06.28	2008.02.13	PALSAR L-band	HH	230	1538.75
2	2008.02.13	2008.03.30	PALSAR L-band	HH	46	25.75
3	2008.05.15	2008.06.30	PALSAR L-band	HH	46	−2446.24
4	2008.05.15	2008.06.30	PALSAR L-band	HV	46	−2446.24
5	2006.12.31	2007.02.17	Radarsat-1 C-band	HH	48	−203.48
6	2007.12.26	2008.01.19	Radarsat-1 C-band	HH	24	254.18

Supplementary material. When the wetlands are divided by levees or rivers, which can be commonly found in Louisiana, the water level changes among the divided wetlands (or water bodies) can be different. Therefore, a single vertical reference is needed to estimate the absolute water level change for each wetland body. Our method of integrating InSAR and altimetery is to obtain the absolute water level change

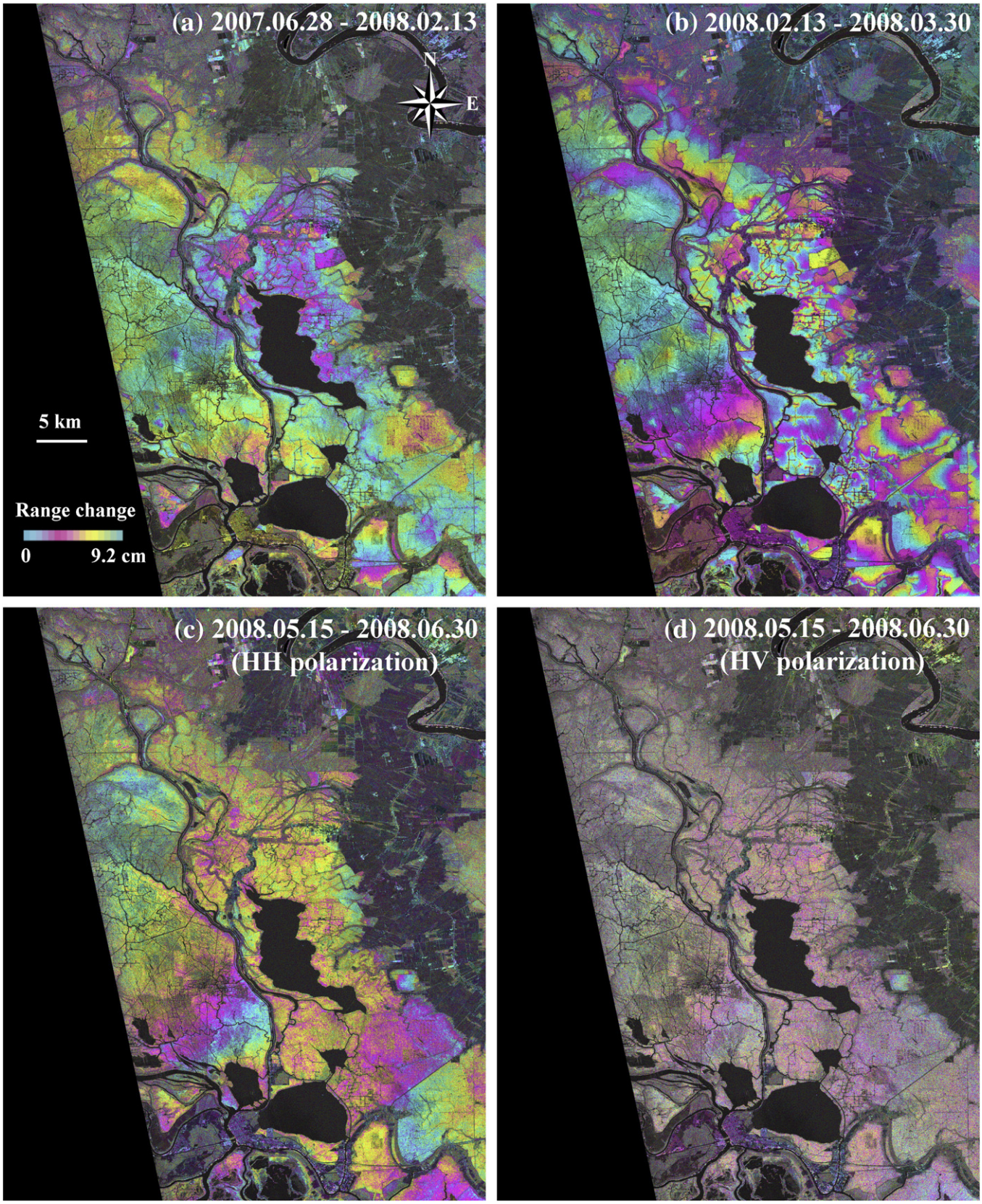

Fig. 2. Wrapped interferograms after removing topographic phase, baseline errors and noise using PALSAR images (a) Jun 28 2007–Feb 13 2008, (b) Feb 13 2008–Mar 30 2008, (c) May 15 2008–Jun 30 2008 (HH polarization), (d) May 15 2008–Jun 30 2008 (HV polarization), and Radarsat-1 images (e) Dec 31 2006–Feb 17 2007, (f) Dec 26 2007–Jan 19 2008.

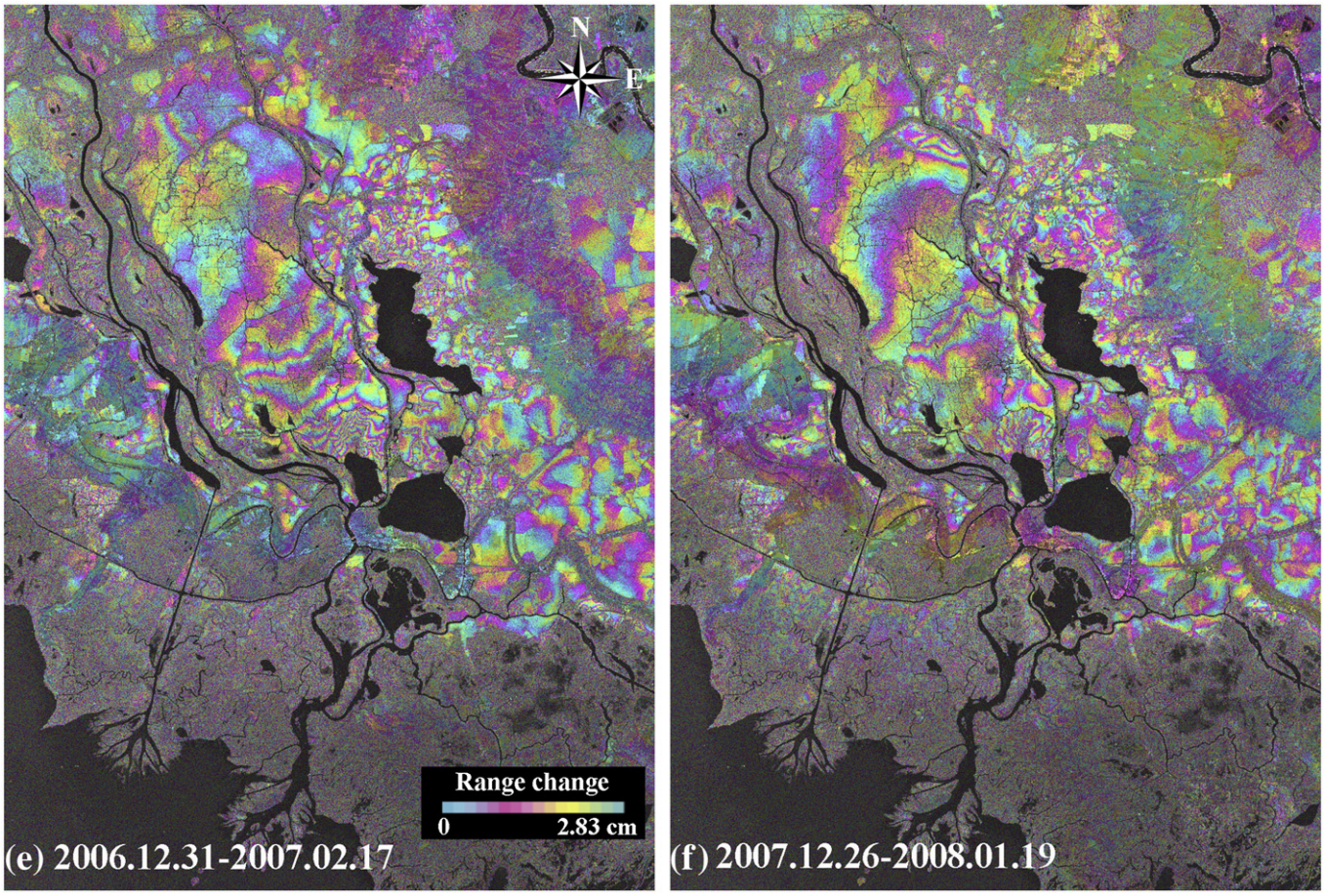

Fig. 2 (*continued*).

measurements from ENVISAT altimeter and use these to construct the absolute water level changes from InSAR.

4. Results

4.1. InSAR processing and coherence/polarimetric analysis

First of all, co-registration of two SAR images, acquired at different times (master and slave data), is performed based on the correlation between the intensities (Rosen et al., 2000; Sheiber & Moreira, 2000). After differencing the co-registered SAR images, the interferogram is generated. The topographic phase is simulated from 30-m resolution C-band Shuttle Radar Topography Mission (SRTM) DEM and removed from the interferogram. The noise is also minimized by applying box-car and band pass filtering. Both PALSAR and Radarsat-1 images are deteriorated by the baseline errors due to inaccurate SAR satellite orbit information (Hanssen, 2000). Using fringe patterns over agriculture fields and urban areas, we estimated the best-fitting polynomial coefficients, which were used to remove the artifacts due to the baseline error. Fig. 2 illustrates the wrapped differential interferograms which contain primarily the displacement phase, and the corresponding coherences are shown in Fig. 3.

The mean coherences shown in Fig. 3 are calculated over the swamp forest classified as in Fig. 1 while excluding agricultural field, water channel, or upland forest. As can be seen from Fig. 3, PALSAR has generally higher coherence than Radarsat-1. It could be due to the difference in their wavelengths as SAR signals with L-band (PALSAR) can penetrate vegetation deeper than C-band (Radarsat-1) signal. In Fig. 3(b), it can also be seen that the L-band coherence decreases as the absolute value of perpendicular baseline ($|B_{perp}|$) increases. Although we cannot make a conclusion based on two Radarsat-1 pairs, Lu and Kwoun (2008) observed no dependence of coherence on baselines less than 350 m. Another interesting point shown in Fig. 3(b) is the coherence difference between InSAR pairs with different polarizations. As PALSAR provides fine beam dual-polarization (FBD) mode, which acquires SAR images from both HH and HV polarizations contrary to fine beam single-polarization (FBS) mode using only HH polarization, the InSAR pair generated from the SAR scenes acquired on May 15 2008 and June 30 2008 are obtained by using two different HH and HV polarizations. It can be seen from Fig. 3 that the InSAR pairs using HH and HV polarization have about 0.4 and 0.1 coherence, respectively. As Lu and Kwoun (2008) concluded that VV polarized ERS-1/2 images have lower coherence than HH polarized Radarsat-1 images, our result confirms that HH polarization is optimal for wetland application of InSAR.

The co-polarized ratio, HH/HV ratio, can indicate the occurrence of double-bounce backscattering in the swamp forest. In general, the value of HH/HV increases constantly as double-bounce backscattering term increases (Freeman & Durden, 1998). It is due to the fact that HH and HV polarizations are sensitive to double-bounce and volume backscattering, respectively. The area shown in Fig. S3, Supplementary material is composed of swamp forest, fresh marsh, agricultural field, and upland forest. As shown in Fig. S3(b), Supplementary material, most of the swamp forest shows relatively high HH/HV ratio (0.4–1.0) indicated as red or yellow colours. This indicates that the primary scattering mechanism is the double-bounce backscattering. On the other hand, the upland forest is dominated by the volume scattering and thus it has small HH/HV. Buildings and cultivated areas in the

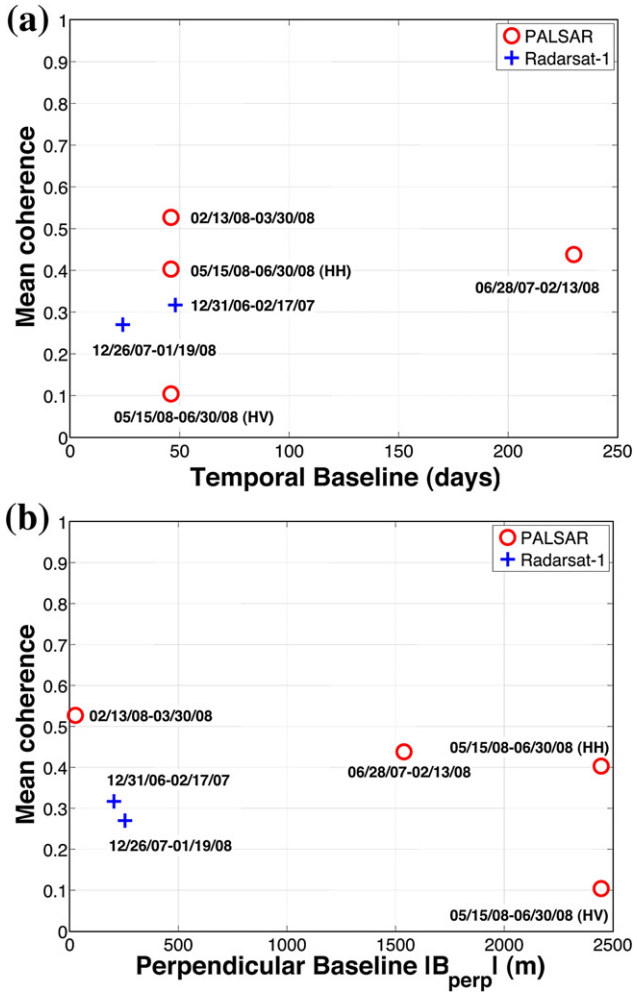

Fig. 3. Mean coherences over the swamp forest of InSAR pairs with respect to (a) temporal baseline (days) (b) perpendicular baseline (m).

agricultural field (i.e., harvested sugar cane field) show high ratio due to corner reflection and the similar scattering characteristics of HH and HV over the bare earth, respectively. Fresh marsh also shows double-bounce backscattering, but its strength is smaller than that of the swamp forest. This simple HH/HV ratio can help land surface classification in wetland because it enables us to identify the scattering characteristic.

Goldstein adaptive filtering (Goldstein & Werner, 1998) is further applied to reduce the noises in the interferogram, and the minimum cost flow (MCF) method (Costantini, 1998) is used for phase unwrapping. However, a priori information about the study area, the Atchafalaya Basin, is necessary for precise phase unwrapping with no phase jumps. Plenty of levees constructed to prevent flooding can be found in the basin, and this can result in different water level change patterns over the separated water bodies. A priori information is that area A shown in Fig. 4 has smaller number of water channels which yield relatively wide and simple fringe patterns whereas area B has more water channels which yield relatively narrow and complex fringe patterns. Generally, complex and steeply wrapped fringe can cause the phase jump, which is a critical error in the procedure of phase unwrapping. To overcome the phase jump, the phase unwrapping of areas A and B is done separately. Specifically, the small water channels in area B, which can cause the phase jump, have been masked out. The final unwrapped interferograms in areas A and B are merged into one interferogram as shown in Fig. 4.

4.2. Water level change from ENVISAT altimetry

Fig. 5 illustrates the 18-Hz nominal ENVISAT ground track over the study area. Background is Landsat ETM+ band 4 (near-infrared) image, and it can help to classify different land cover types such as swamp forests, agricultural field, and open river channel along with the thematic map shown in Fig. 1. Fig. 6 shows the profiles of absolute water level changes from ENVISAT altimetry corresponding to a–d and e–j sections in Fig. 5. Due to the different repeat periods of the satellites (ENVISAT: 35 days, PALSAR: 46 days, Radarsat-1: 24 days), ENVISAT measurements are interpolated to estimate the water level changes between the InSAR pair acquisition dates along each 18-Hz ENVISAT nominal ground track. It can be seen from Fig. 6(a) that the surface elevation along section a–b shows large variation. This is due to the fact that the radar signal is backscattered from the agricultural field as can be seen from Figs. 1 and 5, which may result in spurious height changes. Furthermore, the surface height changes along most parts of section b–c can be influenced by the nearby agricultural field due to the large altimeter footprint (~2 km in diameter over flat surface). Hence, the water level changes over section c–d, which is apparently over the swamp forest, are chosen to be the vertical reference in area B. On the other hand, larger water level variation is observed along sections e–f and i–j, which cover edges of the swamp forest (Fig. 6(b)). It can be seen from Fig. 5 that those sections include not only the swamp forest but also the levee and open river channel. Therefore, the water level changes along the section g–h are selected to be used as the vertical reference over area A. According to Lee et al. (2009), the root-mean-squared errors (RMSEs) between altimetry and *in situ* gauge time series are 20–40 cm over the swamp forest.

4.3. Integration of InSAR and altimetry

Unwrapped interferograms in Fig. 4 can only provide the gradient of water level changes between the InSAR acquisition times. Only the difference between the neighboring pixels can be used to estimate the surface displacement due to water level changes. Thus, the vertical reference is needed to convert the relative water level change to absolute water level change. Water level gauge data are the ideal data source to be the vertical reference; however, water level gauges are sparsely distributed and most of them are located in the river channel, and not in the wetlands. Blue dots in Fig. 7 indicate the selected ENVISAT altimetry points, which are averaged to be used as the vertical references for areas A and B $\left(\left(\frac{dh_0}{dt}\right)_A, \left(\frac{dh_0}{dt}\right)_B\right)$. These are used to generate the high-resolution (~40 m) absolute water level change maps shown in Fig. 7. As can be seen from Fig. 6, areas A and B have different patterns of absolute water level change. Specifically, from Fig. 7(b), while area A has the water level change between 70 and 90 cm, the variation in area B ranges between 10 and 30 cm. The difference can be due to the existence of a levee between areas A and B, which blocks the water flow between them. Future work will incorporate the absolute water level measurements from the altimeter as well as the water level gradients from the altimeter to calibrate InSAR water level measurements.

The absolute water level changes estimated from the integration of InSAR and altimetry can be validated by the water level gauges. Red dots in Fig. 7 indicate the locations of the water level gauges. Old river gauge is located at the Atchafalaya River channel, and Verret gauge is located within the swamp forest in area B. Therefore, the Verret gauge can be used for the direct comparison in area B. Although the Old river gauge is located along the river channel, the comparison in area A is also attempted. The absolute water level changes at or near the gauges can be estimated from interferograms and Eq. (3). The absolute water level changes, $\frac{dh_{\text{Old river}}}{dt}$ and $\frac{dh_{\text{Verret}}}{dt}$ at the Old river gauge and the Verret gauge can be estimated using $\left(\frac{dh_0}{dt}\right)_A$ and $\left(\frac{dh_0}{dt}\right)_B$, respectively. As the Old river gauge is not located within the swamp forest, the absolute water

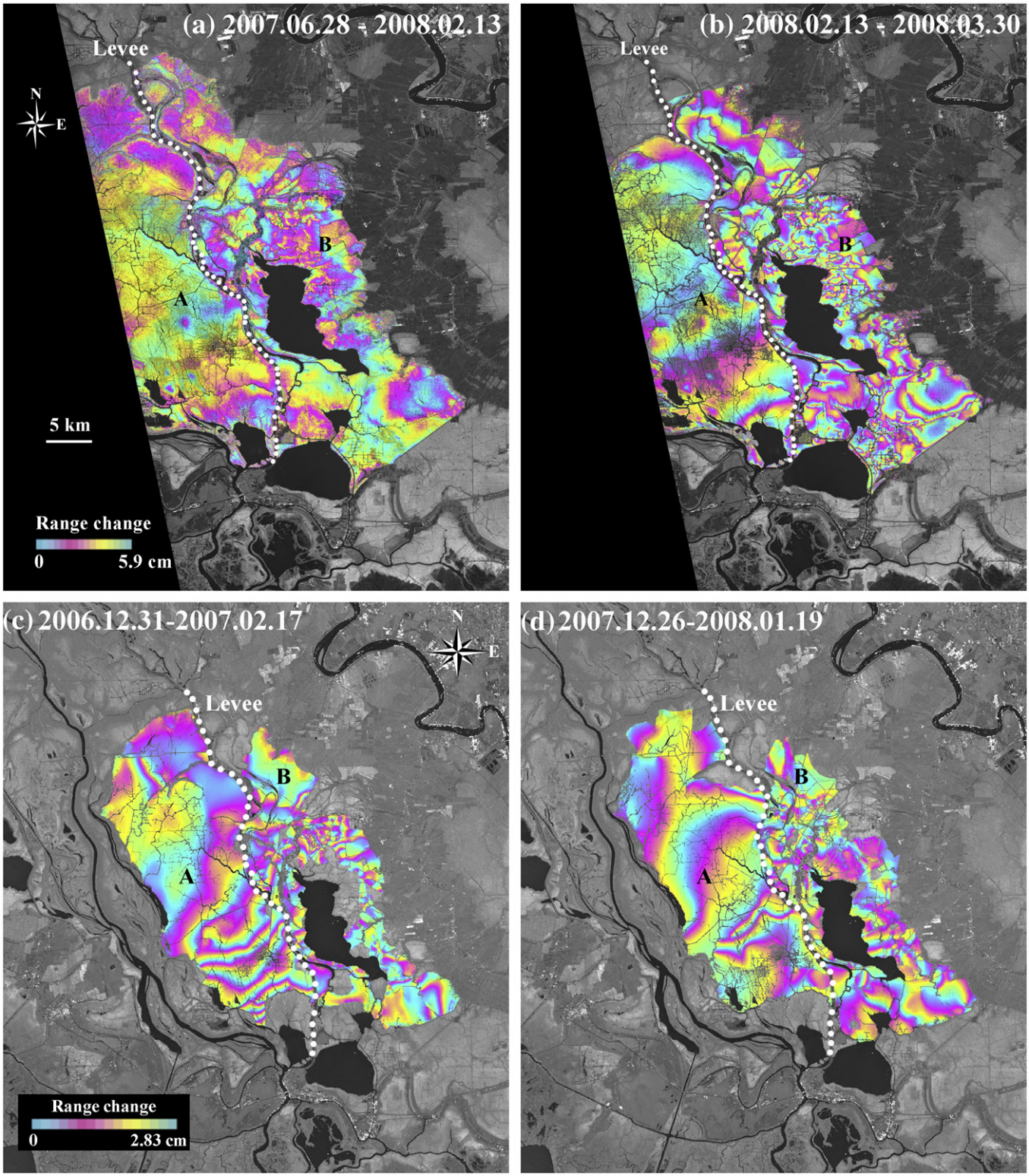

Fig. 4. Unwrapped interferograms over the swamp forest from (a)–(b) PALSAR, and (c)–(d) Radarsat-1 InSAR. White dotted line indicates the levee separating the areas A and B.

level change at the nearest pixel is used to be compared. The differences between the water level gauge measurements and the absolute water level changes from our integration method are shown in Table 2. It is remarkable to see that the differences at the Verret gauge are 2.23, 0.14, and 1.67 cm between the gauge data and the InSAR/altimetry integrated measurements. It is also interesting to see that the Radarsat-1 C-band InSAR provided a commensurate accuracy with the PALSAR L-band InSAR. Although the water level changes at the Old river gauge do not agree well as expected, they reveal the different water level changes in areas A and B. Specifically, during the time interval between Feb 13 2007 and March 30 2008, the water level at the Verret gauge shows decrease as much as 1.53 cm whereas it

increases as much as 124.05 cm at the Old river gauge. This difference can demonstrate that a single vertical reference cannot be used in the wetlands which are divided by the levees or river channels.

5. Discussion and conclusions

The wetland in coastal Louisiana has suffered from frequent flooding and severe storms, and has lost its area due to human activities and natural subsidence. Water level gauge networks located in open river channels cannot help monitor the water level change beneath the swamp forest due to the spatial variations in water level change. Our integration of InSAR and altimetry has been demonstrated to be useful to generate the high-resolution absolute water level change maps over the swamp forest. The conclusion of this study can be summarized as follows:

1. The integration of InSAR and altimetry provides high-resolution absolute water level change maps. If more InSAR pairs are used, denser time series of water level maps can be generated.
2. 18-Hz retracked ENVISAT radar altimetry data can play a role as the vertical reference to covert the relative water level change to the absolute water level change. However, the radar return can be contaminated by the signals from open water or human structures due to its large footprint.
3. The absolute water level changes obtained from C-band InSAR show commensurate accuracy with the water level change observed by L-band InSAR. C- and L-band SAR images have their own advantages and disadvantages. L-band data have deeper penetration depth in the swamp forest and consequently maintain higher coherence, but they are more vulnerable to ionosphere refraction errors. C-band SAR images are less coherent, but also less influenced by the ionosphere effect. As both C- and L-band InSAR images can be utilized, we can estimate water level changes using either or both frequency SAR sensors together with radar altimetry.
4. Our study shows that PALSAR HH polarization obtains higher coherence over the swamp forest than the PALSAR HV polarization mode. Generally, HH polarization is more sensitive to the double-bounce backscattering while HV polarization is more susceptible to the volume scattering inside the canopy. Therefore, HH polarization is preferred for wetland application of InSAR.

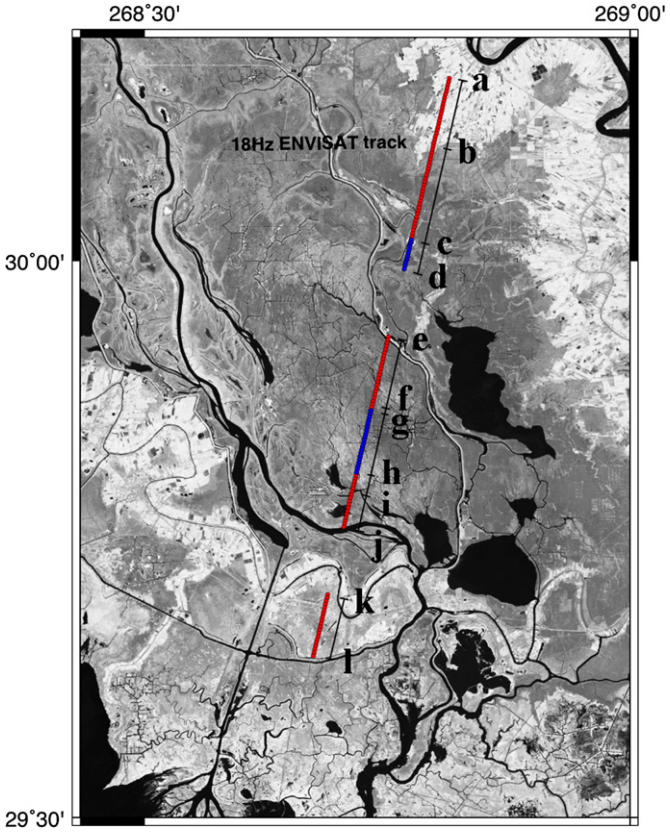

Fig. 5. 18-Hz ENVISAT altimetry nominal ground track over the study area. Background is Landsat ETM+ band 4 image. Blue dots indicate the altimetry data points used for integration with InSAR. (For interpretation of the references to colour in this figure legend, the reader is referred to the web version of this article.)

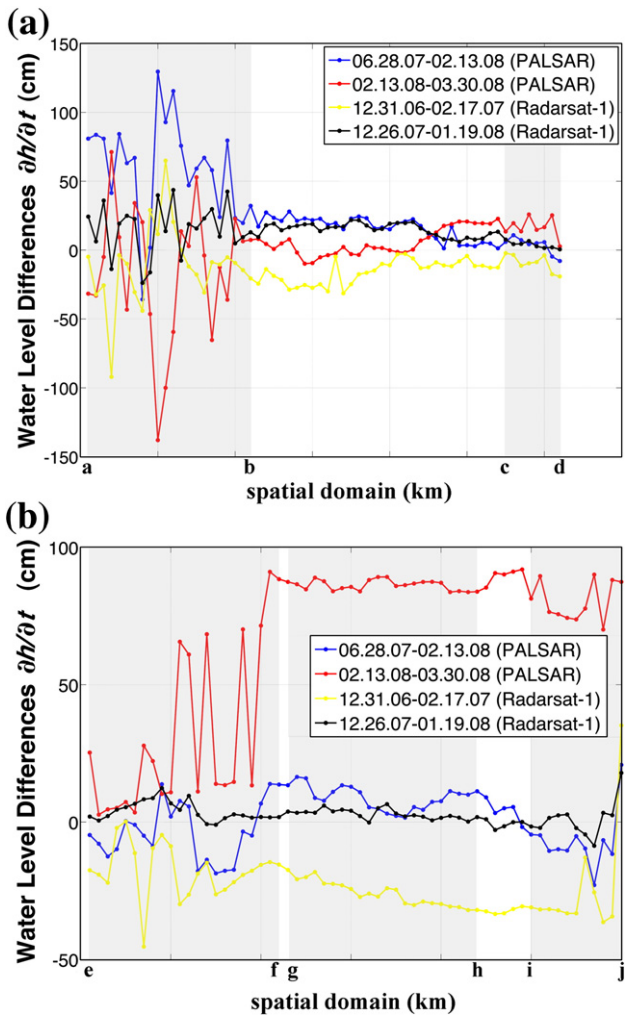

Fig. 6. Absolute water level changes from ENVISAT altimetry. The water level changes are interpolated to be correspondent to InSAR acquisition dates. (a) Profile of water level changes along section a–d shown in Fig. 5. (b) Profile of water level changes along section e–j shown in Fig. 5.

Acknowledgements

This research is partially supported by grants from The National Geospatial-Intelligence Agency's University Research Initiatives Program: HM1582-07-1-2024, National Science Foundation Hydrology program: EAR-0440007, The Climate, Water, and Carbon Program at the Ohio State University, and the U.S. Geological Survey Land Remote Sensing Program. PALSAR and Radarsat-1 data are copyrighted by JAXA/METI 2006-2008 and Canadian Space Agency 2006-2008, and

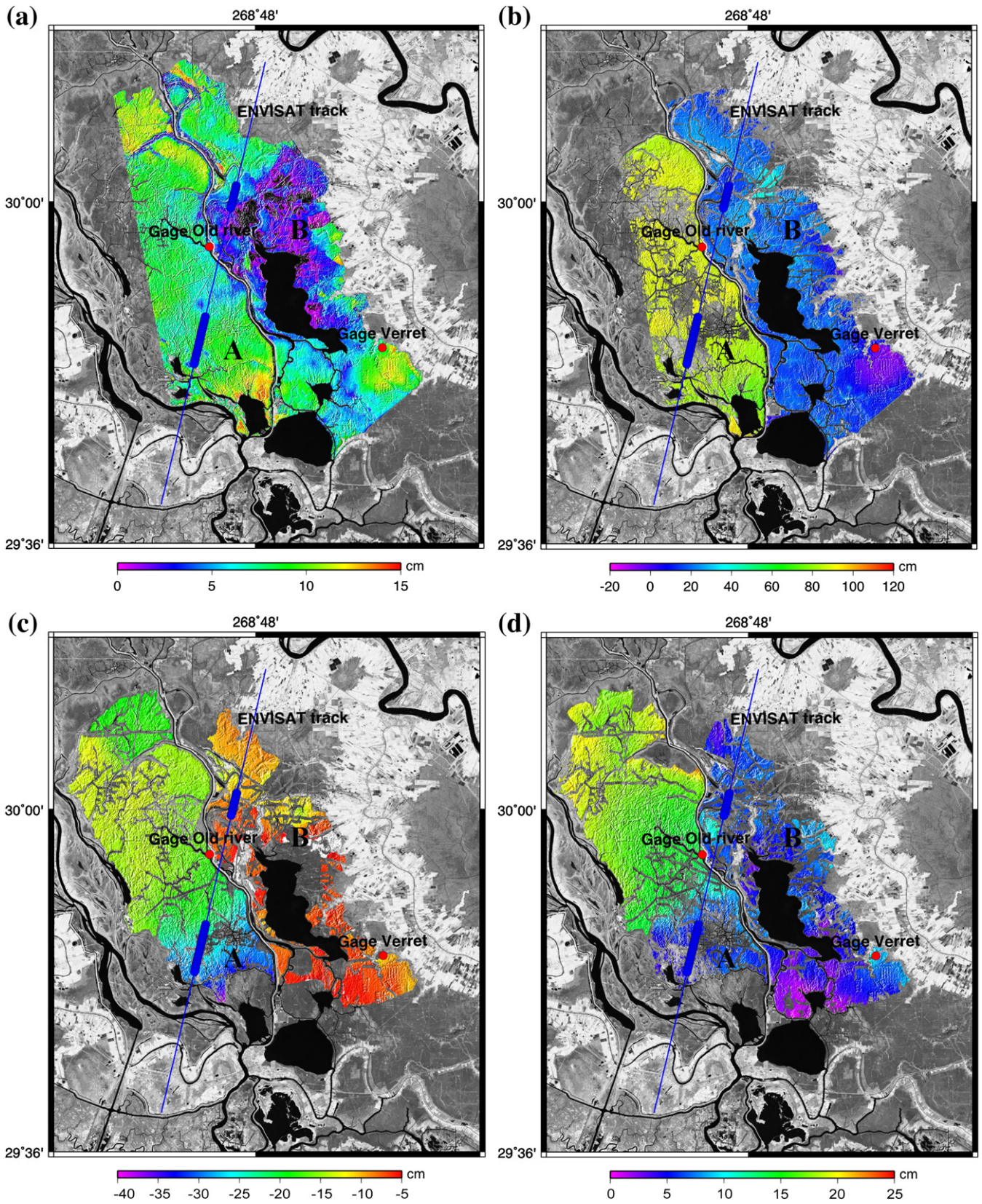

Fig. 7. Maps of the absolute water level change over the swamp forest generated from the integration of ENVISAT altimetry with PALSAR L-band InSAR (a) Jun 28 2007–Feb 13 2008, (b) Feb 13 2008–Mar 30 2008, and Radarsat-1 C-band InSAR (c) Dec 31 2006–Feb 17 2007, (d) Dec 26 2007–Jan 19 2008. Blue line is the altimetry track and the blue dots indicate the data points used as the vertical reference. Red dots show the locations of water level gauges. Old river gauge is located in the river channel and Verret gauge is located within the swamp forest. (For interpretation of the references to colour in this figure legend, the reader is referred to the web version of this article.)

Table 2
Comparisons of the absolute water level changes from water level gauge data and InSAR/Altimeter method between InSAR acquisition times.

Date	Sensor	$\frac{dh}{dt}$ at Verret (gauge)	$\frac{d\hat{h}}{dt}$ at Verret	Difference	$\frac{dh}{dt}$ at Old river (gauge)	$\frac{d\hat{h}}{dt}$ at Old river	Difference
2007.06.28–2008.02.13	PALSAR/ENVISAT altimetry	6.38	8.60	−2.23	3.96	2.69	1.27
2007.02.13–2008.03.30	PALSAR/ENVISAT altimetry	−1.53	−1.39	−0.14	124.05	83.84	40.21
2006.12.31–2007.02.17	Radarsat-1/ENVISAT altimetry	NA	−10.97		NA	−17.80	
2007.12.26–2008.01.19	Radarsat-1/ENVISAT altimetry	7.26	8.94	−1.67	1.22	13.36	−12.14

$\frac{dh}{dt}$ is the absolute water level change from the water level gauge and $\frac{d\hat{h}}{dt}$ is the absolute water level change estimated from the integration of InSAR and altimetry.
Unit:cm.

were provided by Alaska Satellite Facility. ENVISAT radar altimetry data were provided by ESA/ESRIN.

Appendix A. Supplementary data

Supplementary data associated with this article can be found, in the online version, at doi:10.1016/j.rse.2009.06.014.

References

Alsdorf, D., Melack, J., Dunne, T., Mertes, L., Hess, L., & Smith, L. (2000). Interferometric radar measurements of water level changes on the Amazon floodplain. *Nature*, *404*, 174−177.

Alsdorf, D., Smith, L., & Melack, J. (2001). Amazon floodplain water level changes measured with interferometric SIR-C radar. *IEEE Transactions on Geoscience and Remote Sensing*, *39*, 423−431.

Bamber, J. L. (1994). Ice sheet altimeter processing scheme. *International Journal of Remote Sensing*, *15*, 925−938.

Benveniste, J. (2002). *ENVISAT RA-2/MWR product handbook*. Issue 1.2, PO-TN-ESR-RA-0050 Frascati, Italy: European Space Agency.

Berry, P. A. M., Garlick, J. D., Freeman, J. A., & Mathers, E. L. (2005). Global inland water monitoring from multi-mission altimetry. *Geophysical Research Letters*, *32*, L16401. doi:10.1029/2005GL022814.

Birkett, C. M. (1995). The contribution of TOPEX/POSEIDON to the global monitoring of climatically sensitive lakes. *Journal of Geophysical Research*, *100*, 25179−25204.

Birkett, C. M. (1998). Contribution of the TOPEX NASA radar altimeter to the global monitoring of large rivers and wetlands. *Water Resources Research*, *34*, 1223−1239.

Birkett, C. M., Mertes, L. A. K., Dunne, T., Costa, M. H., & Jasinski, M. J. (2002). Surface water dynamics in the Amazon Basin: Application of satellite radar altimetry. *Journal of Geophysical Research*, *107*. doi:10.1029/2001JD000609.

Costantini, M. (1998). A novel phase unwrapping method based on network programming. *IEEE Transactions on Geoscience and Remote Sensing*, *36*, 813−821.

Frappart, F., Calmant, S., Cauhopé, M., Seyler, F., & Cazenave, A. (2006). Preliminary results of ENVISAT RA-2-derived water levels validation over the Amazon Basin. *Remote Sensing of Environment*, *100*, 252−264.

Freeman, A., & Durden, S. L. (1998). A three-component scattering model for polarimetric SAR data. *IEEE Transactions on Geoscience and Remote Sensing*, *36*, 963−973.

Goldstein, R. M., & Werner, C. L. (1998). Radar interferogram filtering for geophysical applications. *Geophysical Research Letters*, *25*, 4035−4038.

Hanssen, R. F. (2000). Radar interferometry: Data interpretation and error analysis: Kluwer Academic Publishers.

Lee, H., Shum, C. K., Yi, Y., Braun, A., & Kuo, C. -Y. (2008). Laurentia crustal motion observed using TOPEX/POSEIDON radar altimetry. *Journal of Geodynamics*, *46*, 182−193. doi:10.1016/j.jog.2008.05.001.

Lee, H., Shum, C. K., Yi, Y., Ibaraki, M., Kim, J. -W., Braun, A., Kuo, C. -Y., & Lu, Z. (2009). Louisiana wetland water level monitoring using retracked TOPEX/POSEIDON altimetry. *Marine Geodesy*, *32*, 284−302.

Lu, Z. (2007). InSAR imaging of volcanic deformation over cloud-prone areas – Aleutian Islands. *Photogrammatric Engineering & Remote Sensing*, *73*, 245−257.

Lu, Z., Crane, M., Kwoun, O. -I., Wells, C., Swarzenski, C., & Rykhus, R. (2005). C-band radar observes water level change in swamp forests. *EOS*, *86*, 141−144.

Lu, Z., Kim, J. -W., Lee, H., Shum, C. K., Duan, J. B., Ibaraki, M., Akyilmaz, O., & Read, C. H. (2009). Helmand River hydrologic studies using ALOS PALSAR InSAR and ENVISAT altimetry. *Marine Geodesy*, *32*, 320−333.

Lu, Z., & Kwoun, O. -I. (2008). Radarsat-1 and ERS InSAR analysis over southeastern coastal Louisiana: Implications for mapping water-level changes beneath swamp forests. *IEEE Transactions on Geoscience and Remote Sensing*, *46*, 2167−2184.

Morris, C. S., & Gill, S. K. (1994). Evaluation of the TOPEX/POSEIDON altimeter system over the Great Lakes. *Journal of Geophysical Research*, *99*, 24527−24539.

Rosen, P., Hensley, S., Joughin, I. R., Li, F. K., Madsen, S. N., Rodriguez, E., & Goldstein, R. M. (2000). Synthetic aperture radar interferometry. *Proceedings of IEEE*, *88*, 333−380.

Sheiber, R., & Moreira, A. (2000). Coregistration of interferometric SAR images using spectral diversity. *IEEE Transactions on Geoscience and Remote Sensing*, *38*, 2179−2191.

Wdowinski, S., Amelung, F., Miralles-Wilhelm, F., Dixon, T., & Carande, R. (2004). Space-based measurements of sheet-flow characteristics in the Everglades wetland, Florida. *Geophysical Research Letters*, *31*, L15503. doi:10.1029/2004GL020383.